Research Article

Journal of Applied Toxicology

Received: 12 March 2012, Revised: 12 April 2012, Accepted: 10 May 2012 Published online in Wiley Online Library: 7 September 2012

(wileyonlinelibrary.com) DOI 10.1002/jat.2782

DNA damage kinetics and apoptosis in ivermectin-treated chinese hamster ovary cells

Gabriela Molinari,[a] Maciej Kujawski,[b] Anna Scuto,[c] Sonia Soloneski[a] and Marcelo L. Larramendy[a]*

ABSTRACT: A comet assay was used to analyze DNA damage kinetics in Chinese hamster ovary (CHO-K1) cells induced by antiparasitic ivermectin (IVM) and the IVM-containing technical formulation Ivomec® (IVO; 1% IVM). Cells were treated with 50 μg ml^{-1} IVM and IVO for 80 min, washed and re-incubated in antiparasiticide-free medium for 0–24 h until assayed using the single-cell gel electrophoresis assay (SCGE). Cell viability remained unchanged up to 3 h of incubation. After 6 h of treatment, cell survival decreased up to 75% and 79% in IVM- and IVO-treated cultures, respectively, remaining unchanged within 12–24 h after treatment. For both anthelmintics, biphasic behavior in DNA damage occurred during the incubation time. A time-dependent increase of IVM- and IVO-induced DNA damage was observed within 0 to 3 h after pulse treatment, revealed by a progressive decrease of undamaged cells and an increase in slightly damaged and damaged cells. Finally, a time-dependent decrease in IVM- and IVO-induced DNA damage was revealed by a progressive decrease of slightly damaged cells and the absence of damaged cells simultaneously with an increase in the frequency of undamaged cells during the final 18 h of incubation. Flow cytometry analysis revealed that both compounds are able to induce a marked increase in early and late apoptosis. Based on our observations, we could conclude that the decrease in DNA lesions is mostly related to IVM-induced cytotoxicity rather than attributable to a repair process. Copyright © 2012 John Wiley & Sons, Ltd.

Keywords: CHO-K1 cells; comet assay; flow cytometry; apoptosis; ivermectin; Ivomec®

INTRODUCTION

Avermectins originated in 1974 at the Kitasato Institute in Japan (http://www.kitasato.ar.jp) when the new species of actinomycete *Streptomyces avermectinius* isolated from soil was found to have an exceptional anthelmintic property (Burg and Stapley 1989; Kita *et al*., 2007; Ŏmura and Crump 2004). The active biocide was isolated in 1975 and was named avermectin (Burg *et al*., 1979; Egerton *et al*., 1979; Miller *et al*., 1979; Ŏmura 2008; Woods and Williams 2007). However, avermectins consist of 16 macrocyclic polyketides that possess excellent biocidal activity with not only a good potency and broad spectrum of activity against a variety of nematode, insect and arachnid parasites (but without antibacterial and antifungal activity), but also with a low level of side effects on the host organism, both in humans and animals (Miller *et al*., 1979).

The chemical structure of avermectins contains a series of pentacyclic macrolactones attached to a disaccharide of the methylated deoxysugar L-oleandrose on C-13. The fermentation of the soil-dwelling *S. avermectinius* produces a mixture of eight different avermectins, which comprise four pairs of homolog compounds namely, A_{1a} and A_{1b}, A_{2a} and A_{2b}, B_{1a} and B_{1b}, and B_{2a}, and B_{2b}. Each pair contains a major component (the a-component) and a minor one (the b-component). Products of the B-series, characterized for possessing a 5′-hydroxy group, are markedly more active than those of the A-series, which contain a 5′-methoxy group instead (Pitterna *et al*., 2009; Wei *et al*., 2005; Zhang *et al*., 2006; Yoon *et al*., 2004). However, it has been demonstrated that 1- and 2-series products exert a similar activity against many parasites (Sunazuka *et al*., 2003). In 1981, the antibiotic was refined by a reduction in the 22,23-olefin of the most active avermectins, namely, B_{1a} and B_{1b}. The obtained 22,23-di-hydro B_1 complex (mixture of 80% B_{1a} and 20% B_{1b}) was developed and marketed as a veterinary drug under the generic and non-proprietary name ivermectin (IVM) (Chabala *et al*., 1980; Ŏmura 2008). The unique ability of IVM is to exert its biocidal activity not only against the ectoparasites, but also the endoparasites, resulting in being the first so-called 'endectocides' agent (Ŏmura and Crump 2004) and becoming the most successful systemic antiparasitic agent ever produced (Campbell *et al*., 1983; Chabala *et al*., 1980; Kita *et al*., 2007). Nowadays, IVM is recognized worldwide as one of the most important endoctocide drugs in animal and human health of the past century (http://www.drugs.com).

The U.S. Environmental Protection Agency (USEPA; http://www.epa.gov) has not reached any conclusion about the real classification of this compound in terms of its putative effect on humans and other species. As a result of the lack of both human cancer epidemiology and positive rodent cancer bioassays, data have not been reported. Thus, the International Agency for Research on Cancer (IARC; http://www.iar.fr) has not listed this antibiotic as a carcinogen so far. Furthermore, it also has not been classified

*Correspondence to: Marcelo L. Larramendy, Cátedra de Citología, Facultad de Ciencias Naturales y Museo, Calle 64 Nro. 3, 1900 La Plata, Argentina.
E-mail: marcelo.larramendy@gmail.com

[a]Cátedra de Citología, Facultad de Ciencias Naturales y Museo, Universidad Nacional de La Plata, Calle 64 Nº 3 B1904AMA La Plata, Argentina

[b]Institute at City of Hope Comprehensive Cancer Center, Department of Cancer Immunotherapeutics Beckman Research and Tumor Immunology, Duarte Rd, Duarte, CA, 91010, USA

[c]Beckman Research Institute at City of Hope Comprehensive Cancer Center, Department of Molecular Medicine, Duarte Rd, Duarte, CA, 91010, USA

Journal of Applied Toxicology

by the European Chemical Agency (ECHA; http://www.echa.europa.eu).

Genotoxicity and cytotoxicity studies conducted with IVM using several end points on different cellular systems are scarce. In the Ames test performed with and without rat liver metabolic activation, the results did not produce any noteworthy increase in revertants to histidine prototrophy (Merck and Co. I. TT # 77-8068, Unpublished data). Negative results were reported for the forward mutation induction at the thymidine kinase locus ($TK^{+/-}$ to $TK^{-/-}$) of mouse lymphoma Fischer L5178Y cells (Merck and Co. I. TT # 79-8034, Unpublished data) as well as for unscheduled DNA synthesis in IMR-90 normal human embryonic lung fibroblasts in the presence and absence of rat liver microsomal activation systems (Merck and Co. I. TT # 80-8205, Unpublished data). A number of years ago, Aleksić and Barjaktarović (1993) reported the ability of IVM to induce sister chromatid exchanges on human lymphocytes *in vitro*. However, 2 years later, negative results were reported by the same research team employing the same end point on the same cell type (Aleksić *et al*., 1996). These finding are in accordance with our recent observations indicating that IVM is unable to induce sister chromatid exchanges in Chinese hamster ovary (CHO-K1) cells (Molinari *et al*., 2009). Negative results have also been observed for the induction of apoptosis in rat thymocytes *in vitro* (Korystov *et al*., 1999). On the other hand, we recently reported the induction of cytotoxicity, e.g. decreasing cell viability and the delay of the cell-cycle progression, concomitant with a reduction of the proliferative rate index in IVM-treated CHO-K1 cells (Molinari *et al*., 2009). Similar observations were found when the mitotic index was employed as a end point for cytotoxicity. While no alteration in the mitotic activity of CHO-K1 cells was observed within the 1–10 $\mu g\,ml^{-1}$ concentration range, a marked reduction of about 89% compared with controls was observed when 25 $\mu g\,ml^{-1}$ was titrated into cultures (Molinari *et al*., 2009). In addition, a loss of lysosomal activity as well as an alteration in the energetic cell metabolism induced by the antiparasitic drug were clearly revealed in IVM-treated CHO-K1 cells (Molinari *et al*., 2009). Finally, we analyzed the ability of IVM to induce single-strand DNA breaks using the single-cell gel electrophoresis (SCGE) assay (Molinari *et al*., 2009). Our data show for the first time positive *in vitro* evaluation of single-strand DNA break induction on CHO-K1 cells when treated with a pulse treatment of both IVM or the IVM-containing technical formulation Ivomec® (IVO) (Molinari *et al*., 2009).

In the present study, we analyzed whether mammalian CHO-K1 cells were able to repair the IVM- and IVO-introduced DNA damage on CHO-K1 cells using the SCGE assay. Furthermore, the cellular response in CHO-K1 cells in terms of the induction of apoptosis by the anthelmintics was also assayed.

MATERIALS AND METHODS

Chemicals

Ivermectin (22,23-dihydroavermectin B1; CAS 70288-86-7; purity, ≥90%), ethidium bromide (3,8-diamino-5-ethyl-6-phenylphenanthridinium bromide; CAS 1239-45-8), acridine orange [3,6-bis (dimethylamino)acridine hydrochloride; CAS 65-61-2], agarose (routine use and low melting; CAS 9012-36-6) and dimethyl sulfoxide (DMSO; CAS 67-68-5) were purchased from Sigma Chemical Co. (St. Louis, MO, USA). Annexin V-FITC and propidium iodide were purchased from BD Biosciences (Franklin Lakes, NJ, USA). Ivomec® (1% IVM) was kindly provided by Merial Argentina S.A. (Buenos Aires, Argentina). Bleomycin (BLM; Blocamycin®) was kindly provided by Gador S.A. (Buenos Aires, Argentina).

Cell Cultures and Pesticide Treatment for the SCGE Assay

CHO-K1 cells were grown in Ham's F-10 medium (Gibco, Grand Island, NY, USA) supplemented with 10% fetal calf serum (Gibco), 100 units ml^{-1} penicillin (Gibco) and 100 $\mu g\,ml^{-1}$ streptomycin (Gibco) at 37 °C in a 5% CO_2 atmosphere. Experiments were set up with cultures in the log phase of growth. Prior to drug treatment, cells were detached with a rubber policeman, collected by centrifugation, resuspended in complete culture medium,and then counted. Afterwards, aliquots of 3.5×10^5 cells ml^{-1} were incubated during 80 min at 37 °C in a 5% CO_2 atmosphere in culture medium containing the test compounds. IVM was first dissolved in DMSO and then diluted in culture medium, whereas IVO was diluted directly in culture medium. Both IVM and IVO were diluted so that the addition of 100 µl into the cultures allowed the required concentration to be reached. IVM and IVO were used at the final concentration of 50 $\mu g\,ml^{-1}$. The concentration of the test compounds employed throughout the study corresponds to the nominal concentration of the active ingredient and was selected according to previous results (Molinari *et al*., 2009). The final solvent concentration was lower than 1% for all treatments. Negative controls (untreated cells and solvent vehicle-treated cells) and positive controls (BLM, 10 $\mu g\,ml^{-1}$) were run simultaneously with pesticide-treated cultures. None of the treatments produced significant pH changes in the culture medium. Thereafter, the cells were washed twice with pesticide-free complete culture medium, collected by centrifugation, and resuspended in 1 ml of pesticide-free complete culture medium. The SGCE and cell viability assays were performed immediately after the 80-min treatment or after a post-treatment incubation period of 0–24 h at 37 °C in a 5% CO_2 atmosphere with harvesting times at 0, 0.5, 1, 1.5, 3, 6, 12, 18 and 24 h. Cultures were duplicated for each experimental point in at least three independent experiments. The same batches of culture medium, sera and reagents were used throughout the study.

Cell Viability Assay

At the end of the culture period, cell viability was determined using the ethidium bromide/acridine orange assay as described previously (McGahon *et al*., 1995). Briefly, one aliquot of 5 µl of a 1 : 1 freshly prepared mixture of ethidium bromide (100 $\mu g\,ml^{-1}$) and acridine orange (100 $\mu g\,ml^{-1}$) was mixed with 50 µl of the cell suspension under study. Afterwards, the cells were analyzed using an Olympus BX50 fluorescence photomicroscope equipped with an appropriate filter combination. Viable cells appear green fluorescent, whereas orange-stained nuclei indicate dead cells. At least 500 cells were counted per experimental point from each experiment, and the results were expressed as a percentage of viable cells among all cells.

SCGE Assay

The remaining cell culture (950 µl) was used for microgel electrophoresis. To detect single-strand DNA breaks, the SCGE assay was performed according to the alkaline procedure described by Singh *et al*. (1996) with minor modifications. Slides were cleaned with 100% ethanol and air-dried. Two solutions containing 0.5% normal melting agarose (NMA) and 0.5% low

melting agarose (LMA) solution in Ca^{2+}/Mg^{2+}-free phosphate buffered saline (PBS) were prepared. Seventy-five microliters of NMA were transferred onto a slide, spread evenly and incubated at 37 °C for 20–30 min. Afterwards, 95 μl of LMA together with 7×10^3 cells (20-μl cell suspension plus 75 μl of LMA) was applied, covered with a coverslip and placed at 4 °C for 15 min. After the second layer had solidified, a third layer of 75 μl of LMA was added, and the slides were immersed in ice-cold freshly prepared lysis solution (1% sodium sarcosinate, 2.5 M NaCl, 100 mM Na_2EDTA, 10 mM Tris, pH 10.0, 1% Triton X-100, 10% DMSO) and then lysed in darkness for a 2-h period (4 °C). After lysis, the slides were placed in a horizontal electrophoresis buffer (1 mM Na_2EDTA, 300 mM NaOH, pH 13.0) for 20 min at 4 °C to allow the cellular DNA to unwind, followed by electrophoresis in the same buffer and temperature for 30 min at 0.8 V cm^{-1}. Finally, the slides were neutralized with a solution comprising 0.4 M Tris–HCl, pH 7.5, stained with 4-6-diamino-2-phenylindole (DAPI; Vectashield mounting medium H1200; Vector Laboratories, Burlingame, CA, USA). Slides were coded and scored blind by one cytogeneticist. Analysis of the slides was performed under an Olympus BX50 fluorescence photomicroscope equipped with an appropriate filter combination and an Olympus DP71 high-sensitivity monochrome charge-coupled device camera and automated capture image software. The cellular nucleus diameter and the comet length, determined as the diameter of the nucleus plus migrated DNA, were measured using a calibration scale with an 100× fluorescence objective. The width of the nucleus and comet length (expressed in micrometers) were determined from 50 randomly captured cells per experimental point of each experiment. Two parallel slides were performed for each experimental point. Cells were visually graded into three categories, as described previously (González *et al.*, 2003; Molinari *et al.*, 2009). Depending on the DNA damage level, the categories were as follows: undamaged (no tail comet; diameter ≤ 30 μm), slightly damaged (diameter 31–45 μm) and damaged cells (width and length >45 μm). The results are expressed as the mean values of cells ± standard error (SE) of the mean from each cellular category of three independent experiments.

Cell Cultures and Pesticide Treatment for Flow Cytometry Analysis

Briefly, CHO-K1 cells in the log phase of growth were seeded in 24-well microplates at a density of 3.5×10^4 cells ml^{-1} and treated for 24 h after plating to detect apoptotic and necrotic cells among the cell population. Both IVM and IVO were diluted so that the addition of up to 20 μl into cultures allowed the final concentrations of 10 and 25 μg ml^{-1} to be reached. These concentrations were selected according previous results (Molinari *et al.*, 2009) and related to those doses used commonly in animals (Lifschitz *et al.*, 2007). After an incubation period of 24 h (37 °C, 5% CO_2), cells were processed for flow cytometry using Annexin V-FITC double staining according to the manufacture's protocol. The treated cells were washed with PBS and resuspended in 100 μl of binding buffer, supplemented with 5 μl of FITC-Annexin V and 5 μl of PI, and incubated for 15 min at room temperature in the dark. The cell populations were discriminated as viable (Annexin V negative/PI negative), early-apoptotic (Annexin V positive/PI negative), late-apoptotic (Annexin V positive/PI positive) and necrotic cells (Annexin V negative/PI positive). Flow cytometric analysis was performed with an Accuri C6 flow cytometer (BD Biosciences).

Statistical Analysis

The two-tailed Student's *t*-test was used to compare cell viability data between treated and control cells. The non-parametric Kruskal–Wallis test was used to compare the global effect of a pesticide over control cells, whereas individual comparisons between pairs of data were performed using the Mann–Whitney *U*-test employing SPSS 9.0 software. The relationship between the frequencies of different cell types and harvesting times was evaluated using Spearman's rank order linear correlation test. The level of significance chosen was $P \leq 0.05$ unless indicated otherwise.

RESULTS

As no differences in cell viability and in the frequencies of undamaged/damaged cells revealed by the SCGE assay were observed between untreated and DMSO-treated cells, pooled data are presented for control cultures. BLM pulse treatment did not modify cell viability in regard to negative control values ($P > 0.05$; Fig. 1). Cell viability after a 80-min treatment with 50 μg ml^{-1} IVM or IVO did not show significant changes compared with control values until 3 h of incubation ($P > 0.05$; Fig. 1A, B). However, from 6 to 24 h of incubation, a significant decrease in cell survival was achieved in those IVM- (Fig. 1A) and IVO-treated cultures (Fig. 1B), reaching values as low as 75% to 80% ($P \leq 0.05$ to $P \leq 0.01$).

Results from the SCGE assay showed statistically significant differences between negative and positive controls. BLM pulse treatment produced an enhancement of the frequency of both slightly damaged ($P \leq 0.001$) and damaged cells ($P \leq 0.001$), and a concomitant decrease in the frequency of undamaged cells ($P \leq 0.001$) compared with the corresponding negative control values (Fig. 1).

A clear increase in DNA damage was found immediately after test compound treatments (0 h) (Fig. 1). In both IVM- (Fig. 1A) and IVO-treated cells (Fig. 1B), DNA damage was revealed by a decrease in the proportion of undamaged cells ($P \leq 0.05$ or $P \leq 0.01$) and by an increase in the frequency of both slightly damaged ($P \leq 0.001$) and damaged cells, although the latter did not reach statistical significance ($P > 0.05$). Figure 1 also denotes that for both chemicals, a biphasic behavior in DNA damage kinetics occurred during the time interval between exposure and harvesting, namely, between 0–3 and 6–24 h. A time-dependent increase in IVM- and IVO-induced DNA damage was observed by a progressive decrease of undamaged cells simultaneously with an increase in the frequency of slightly damaged and damaged cells within the 0–3 h post-incubation time. A regression analysis showed that the number of undamaged cells decreased as a function of the incubation time of both IVM- ($r = -0.99$, $P \leq 0.001$; Fig. 1A) and IVO-treated cells ($r = -0.99$, $P \leq 0.001$; Fig. 1B). On the other hand, the number of slightly damaged cells increased as a function of the incubation time of both IVM- ($r = 0.89$, $P \leq 0.001$; Fig. 1A) and IVO-treated cells ($r = 0.99$, $P \leq 0.001$; Fig. 1B), and so did the number of damaged cells ($r = 0.95$, $P \leq 0.001$ and $r = 0.88$, $P \leq 0.001$ for IVM- and IVO-treated cells, respectively).

When the analysis was performed within the 6–24 h incubation time period, a time-dependent decrease of IVM- (Fig. 1A) and IVO-induced DNA damage (Fig. 1B) was observed because of a progressive reduction in slightly damaged cells and the absence of damaged cells simultaneously with an increase in the frequency of undamaged cells during the final 18 h of culture. A regression test showed that the number of slightly damaged cells decreased

Journal of Applied Toxicology

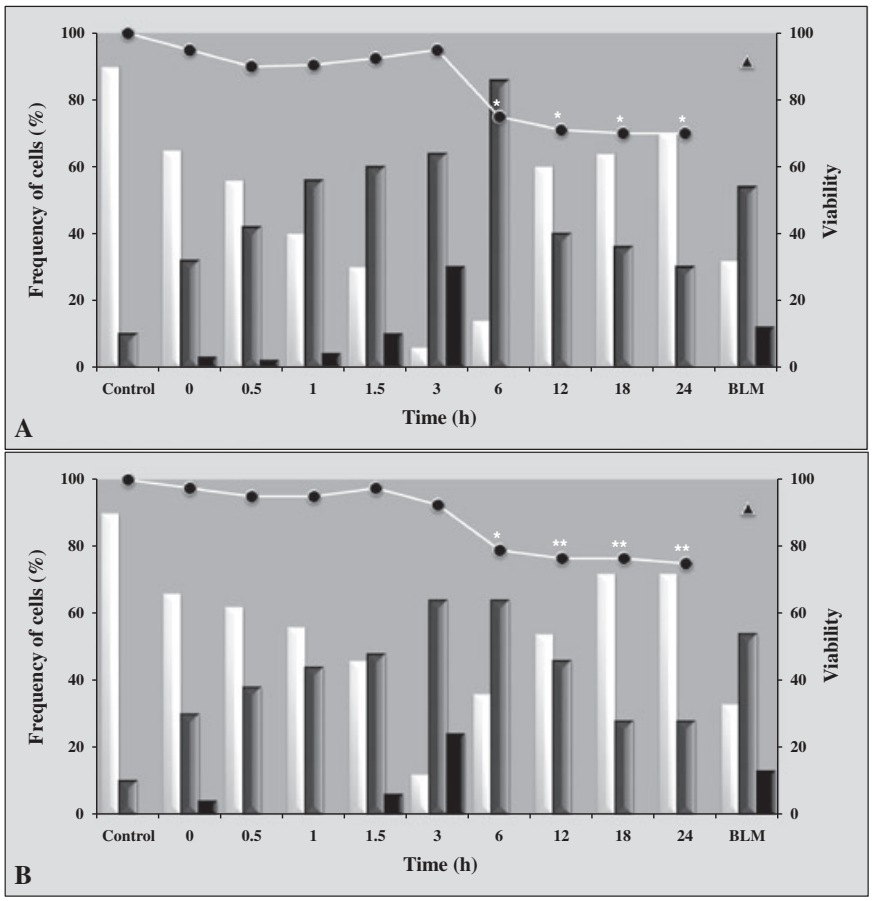

Figure 1. Time course of the *in vitro* DNA damage induced in Chinese hamster ovary (CHO-K1) cells by an 80-min pulse treatment with ivermectin (A; 50 μg ml^{-1}) and the ivermectin-containing technical formulation Ivomec® (B; 50 μg ml^{-1}) detected using the single-cell gel electrophoresis assay (SCGE). Electrophoresis was performed at 4 °C for 30 min at 0.8 V cm^{-1}, and cells were stained with 4-6-diamino-2-phenylindole (DAPI). For each harvesting time, pooled data from three independent experiments were reported as mean nucleoid values ± SE out of a total of 150 randomly selected cells analyzed. According to the level of damage, cells were classified as undamaged (white bars), slightly damaged (grey bars) or damaged (black bars), and their frequencies (*y*-axis) plotted against harvesting times (0–24 h, *x*-axis). Cell viability was determined using the ethidium bromide/acridine orange assay and expressed as the proportion of living cells at different harvesting times after an 80-min pulse treatment. For each harvesting time, pooled data from three independent experiments are reported as mean values ± SE (black circles; *y*-axis) and plotted against incubation time (*x*-axis). Bleomycin (BLM) (10 μg ml^{-1}) was used as a positive control (black triangle). *$P \leq 0.05$; **$P \leq 0.01$.

as a function of the incubation time of both IVM- ($r = -0.88$, $P \leq 0.01$; Fig. 1A) and IVO-treated cells ($r = -0.94$, $P \leq 0.001$; Fig. 1B). Concomitantly, a time-dependent increase in the number of undamaged cells was observed within the 6–24 h culture time in IVM- ($r = 0.88$, $P \leq 0.01$; Fig. 1A) and IVO-treated cultures ($r = 0.94$, $P \leq 0.001$; Fig. 1B). At 24 h after treatment, while no damaged cells were found in IVM- and IVO-pulse-treated cell cultures ($P > 0.05$; Fig. 1), a decrease in the frequencies of slightly damaged cells was found, although not reaching negative control values (Fig. 1).

A Mann–Whitney test demonstrated that the length and width of nuclear DNA from IVM-treated cells immediately after exposure (0 h) were higher (Fig. 2A) and wider (Fig. 2B), respectively, than in control cells ($P \leq 0.05$ and $P \leq 0.001$). When cells were allowed to grow in IVM-free culture medium, a time-dependent increase in the amount of free DNA fragments that could migrate (i.e. a strong enhancement in the average of nuclear DNA length) was observed between 0 and 3 h after treatment ($r = 0.99$; $P \leq 0.001$; Fig. 2A). On the other hand, a time-dependent decrease in nuclear DNA length within the 6–24 h period after the pulse treatment was observed ($r = -0.85$; $P \leq 0.01$; Fig. 2A) as a result of alterations in slightly damaged ($P \leq 0.001$) and undamaged cells ($P \leq 0.001$). Statistical analysis revealed that such a strong increase in nuclear DNA length was specific to both damaged ($P \leq 0.001$) and slightly damaged ($P \leq 0.001$) cells. Similarly, while a time-dependent increase in nuclear DNA width was observed within the 0–3 h post-treatment period ($r = 0.99$; $P \leq 0.001$; Fig. 2B), a time-dependent decrease in nuclear width was found during the 6–24 h period after the pulse treatment ($r = -0.84$; $P \leq 0.01$; Fig. 2B). Overall, the IVM-damaged cell population did not completely recover the features of the control cells even after 24 h post-treatment, with the nuclear DNA from treated cells being longer ($P \leq 0.05$; Fig. 2A) and wider ($P \leq 0.05$; Fig. 2B) than that from control cells.

The length and width of nuclear DNA from IVO-treated cells were larger (Fig. 2C) and wider (Fig. 2D), respectively, than in untreated cells immediately after exposure (0 h; $P \leq 0.05$). A time-dependent increase in the amount of migrating DNA fragments was observed in the 0–3 h period after treatment ($r = 0.98$; $P \leq 0.001$; Fig. 2C). However, a time-dependent decrease in nuclear length was achieved in those cells harvested within the period

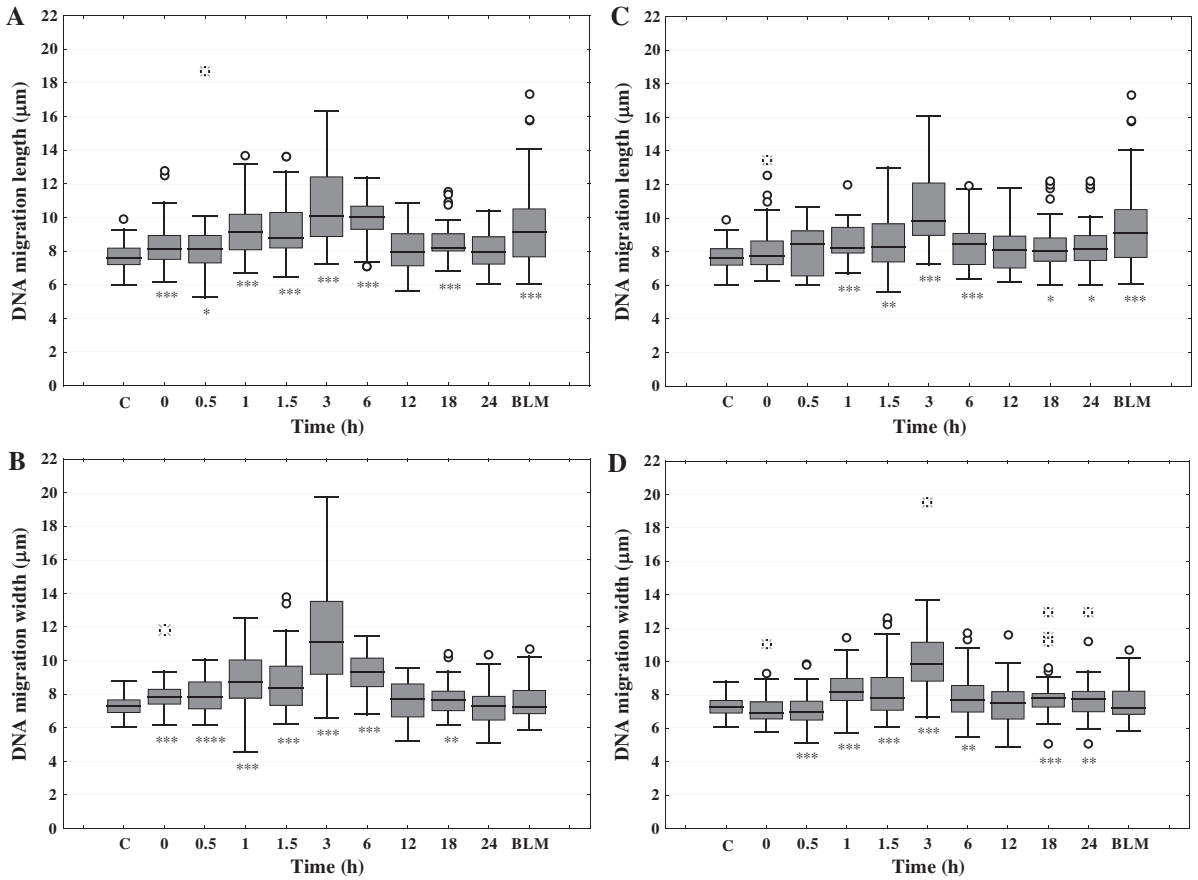

Figure 2. (A–D) Time course of the *in vitro* DNA damage induced in Chinese hamster ovary (CHO-K1) cells using an 80-min pulse treatment with ivermectin (A, B; 50 μg ml^{-1}) and the ivermectin-containing technical formulation Ivomec® (C, D; 50 μg ml^{-1}) detected using the single-cell gel electrophoresis assay (SCGE). Electrophoresis was performed at 4 °C for 30 min at 0.8 V cm^{-1}, and cells were stained with 4-6-diamino-2-phenylindole (DAPI). For each harvesting time, pooled data from three independent experiments were reported, and a total of 150 randomly selected cells were visualized for DNA damage. The nuclear DNA length (A, C) and the nuclear DNA width (B, D) expressed in micrometers (*y*-axis) are plotted against different harvesting times (in hours, *x*-axis). Bleomycin (BLM) (10 μg ml^{-1}) was used as positive control, whereas untreated and dimethyl sulfoxide (DMSO)-treated cells were used negative controls (C; *x*-axis). The data are displayed as box plots, where the *y*-axes show the range data. Each box plot encloses 50% of the data, with the median value of the variable displayed as a line. The top and the bottom of each box mark the limits ± 25% of the variable population. The lines extending from the top and the bottom of each box mark the minimum and maximum values that fall within an acceptable range. Any value outside this range is displayed as an individual point (empty circles). *$P \leq 0.05$; **$P \leq 0.01$; ***$P \leq 0.001$.

6–24 h after the pulse treatment ($r = -0.86$; $P \leq 0.01$; Fig. 2C). Statistical analysis revealed that such a strong increase in nuclear DNA length was specific to both damaged ($P \leq 0.001$) and slightly damaged ($P \leq 0.001$) cells among all cell populations. Similarly, while a time-dependent increase in nuclear DNA width was observed during the 0–3 h post-treatment period ($r = 1.00$; $P \leq 0.001$; Fig. 2D), a time-dependent decrease in nuclear width was found during the 6–24 h period after the pulse treatment ($r = -0.83$; $P \leq 0.01$; Fig. 2D). Overall, the IVO-damaged cell population did not completely achieve the nuclear DNA length ($P \leq 0.05$; Fig. 2C) and the width of the control cells ($P \leq 0.01$; Fig. 2D), even after a 24 h post-treatment time, with the DNA migration appearing longer and wider than in the untreated cell population (Fig. 2C and D, respectively).

Flow cytometry analyses of cells treated with 10 and 25 μg ml^{-1} IVM and IVO are presented in Fig. 3. As no differences in the frequencies of alive, early-apoptotic, late-apoptotic and necrotic cells were found between untreated and DMSO-treated cells, pooled data are presented for control cultures. The results indicate that both IVM and IVO induced early ($P \leq 0.001$) as well as late apoptosis ($P \leq 0.001$). Overall, the regression analyses revealed that the frequency of apoptotic cells increased as a function of the concentrations of both IVM ($r = 0.90$, $P \leq 0.05$) and IVO titrated into cultures ($r = 0.86$, $P \leq 0.05$) (Fig. 3D). Furthermore, both compounds were able to induce an increase in the frequency of necrotic cells compared with control values ($P \leq 0.001$), regardless of the concentration (Fig. 3).

DISCUSSION

In the present study, we employed the alkaline version of the SCGE assay to analyze the damage inflicted by IVM as well as the IVM-based commercial formulation IVO (1% IVM) on the DNA from 80 min pulse-treated CHO-K1 cells during the first 24 h after treatment. In addition, the ethidium bromide/acridine orange fluorescence technique was performed to evaluate cell viability. Furthermore, flow cytometry analysis was also performed to quantitatively determine the percentage of apoptotic and necrotic cells. The results revealed that biphasic behavior in DNA damage kinetics occurred with incubation time, namely, a time-dependent

Journal of AppliedToxicology

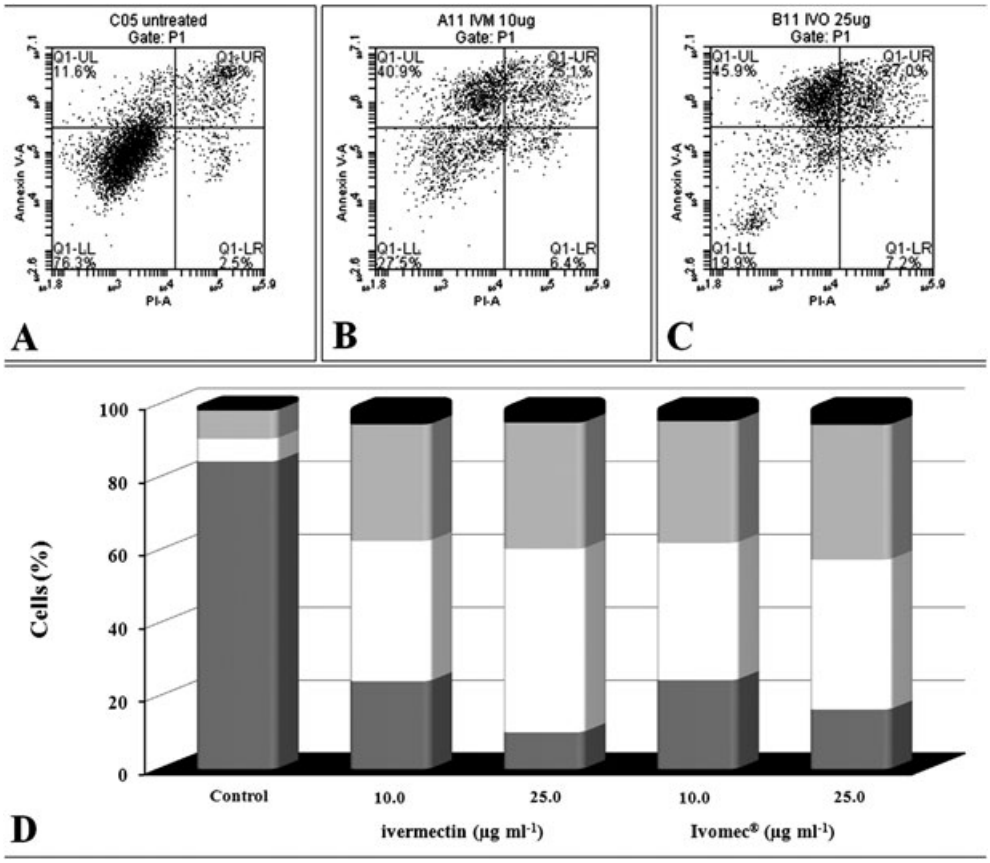

Figure 3. Ivermectin (IVM) and Ivomec® (IVO) induce apoptosis in Chinese hamster ovary (CHO-K1) cells. Cells were treated with test compounds and processed 24 h later with the Annexin V/PI staining for quantification of the incidence of apoptosis cells by flow cytometry. (A–C) Representative dot plot analyses of control (A), 10 µg ml^{-1} IVM-treated (B) and 25 µg ml^{-1} IVO-treated (C) cultures. The cell populations were discriminated in each quadrant as viable cells in the lower left (LL; Annexin V negative/PI negative), early-apoptotic cells in the upper left (UL; Annexin V positive/PI negative), late-apoptotic cells in the upper right (UR; Annexin V positive/PI positive) and necrotic cells in the lower right quadrant (LR; Annexin V negative/PI positive). The percentages of cells from four independent experiments after flow cytometry analysis are shown in (D). Early apoptosis (white bar sections), late apoptosis (light gray bar sections), alive (dark gray bar sections) and necrotic cells (black bar sections) among all cells from IVM- and IVO-treated cell cultures are shown.

increase of IVM- and IVO-induced DNA damage within 0–3 h after treatment and a time-dependent decrease within 6–24 h after pulse treatment. Flow cytometry analysis revealed that both compounds are able to induce a significant concentration-dependent enhancement of both early and late apoptosis as well as, to a lesser extent, necrosis after continuous treatment lasting 24 h.

Previously we reported equivalent levels of DNA damage in CHO-K1 cells induced immediately after an 80-min pulse treatment with 50 µg ml^{-1} IVM and IVO, the concentration employed in the present study (Molinari *et al*., 2009). The present results confirmed our previous observations, corroborating that such concentration of either IVM or IVO resulted in a manifest equivalent level of single-strand DNA break induction in both mammalian (Molinari *et al*., 2009) as well as insect cells (Molinari *et al*., 2010). Furthermore, these findings are in accordance with other previous observations indicating a genotoxic effect exerted by abamectin, the most active form of the avermectins (avermectin B_{1a}), which was found to induce single-strand DNA breaks in rat hepatocytes *in vivo* (USEPA 1989). However, no attempt to analyze the damage kinetics of the induced lesions have been assessed in any of these studies (Molinari *et al*., 2009, 2010; USEPA 1989).

To the best of our knowledge there is no available information on the DNA damage kinetics inflicted by IVM. However, our results could indicate that the macrocyclic lactone or some of its metabolites could require more than 80 min to exert their maximal DNA deleterious effects once the cells became exposed. According to our results, this period could last approximately 3 h after an initial pulse treatment. In accordance with our suggestion, Rodríguez-Mercado *et al*. (2011) recently analyzed, by applying the single cell electrophoresis assay, the DNA damage and repair processes induced in human leukocytes by vanadium (IV) in three oxidation states *in vitro*. The authors reported that vanadium tetraoxide treatment significantly increased the DNA damage starting at 4 or 6 h after treatment, although only 2 h of exposure are required for vanadium(III) trioxide and vanadium(V) pentoxide to produced the same effect (Rodríguez-Mercado *et al*., 2011).

The current comet assay results clearly highlight a time-dependent decrease IN IVM- and IVO-induced DNA damage within 6–24 h after pulse treatment. So far, the exact mechanism(s) of the antiparasiticide-induced DNA damage is not known. It is well documented that the repair kinetic profile of the single-strand breaks induced by active oxygen species, when analyzed by the comet assay, is totally different from the damage kinetic profile

of those IVM- and IVO-induced lesions observed in the present study. In fact, the *in vitro* repair of the former in mammalian cells is extremely rapid, with most of the breaks being resealed within 10 min (Olive *et al.*, 1990). Accordingly, the possibility that IVM- and IVO-inflicted DNA lesions are as a result of delivery of active oxygen species could be ruled out as our experimental conditions clearly demonstrate the requirement of CHO-K1 cells of an approximately 18-h repair process for the resealing of lesions. On the other hand, another plausible explanation could be alkylation of the DNA molecule by this antiparasiticide. It has been demonstrated previously in CHO-K1 cells that single-strand DNA breaks after treatment with different alkylating agents, e.g. *N*-ethyl-*N*-nitrosourea and *N*-ethyl-*N*-nitro-*N*-nitrosoguanidine or fungicides, e.g. bis(dithiocarbamates)zinc (zineb), are long lasting, with repair occurring within a lapse of up to 24 h after pulse treatment (Fortini *et al.*, 1996; González *et al.*, 2003).

In our observations, the IVM- and IVO-induced DNA damage was more severe at 6 than 24 h after treatment. This might indicate that the decrease in the frequency of DNA damage estimated by a reduction in the tailed comets is as a result of a repair of the lesions induced by treatment. Interestingly, our results revealed that when damaged cells were analyzed at the end of the recovering period of 24 h, the resulting cell population did not completely recuperate the morphological features of the control cells, i.e. increased nuclear diameter. The same finding was reported previously by Fortini *et al.* (1996) in CHO-K1 cells after a complete repair of either X-ray- and alkylation-induced DNA damage. Accordingly, these authors proposed that such morphological discrepancies could be attributable to differences in the packaging of DNA in those cells undergoing repair. Furthermore, we made a similar observation when studying the repair process of mammalian cells exposed to the fungicide zineb (González *et al.*, 2003). This fact, together with the time-dependent increase in the frequency of non-migrating cells observed within the 6–24 h period after treatment, could allow us to claim that CHO-K1 cells could be able to repair IVM- or IVO-induced lesions into DNA. In spite of a clear repair of IVM- and IVO-induced DNA damage, the present observations could further characterize the antibiotic with other effects, mostly related to cytotoxicity and cell turnover. Among them can be included the induction of a selective IVM- and IVO-mediated cell death of the most damaged cells, as only a reduced proportion of cells are able to be analyzed at the latest harvesting times. In agreement with this, our results clearly demonstrated that no cells belonging to the damaged type were observed at any harvesting time after 12 h of treatment, but there was a decrease in the proportion of slightly damaged cells. Furthermore, another possibility to explain our observations could be related to an exponential dilution of the damage because of cell division, if the antiparasiticide does not prevent damaged CHO-K1 cells from entering a second cell cycle during the 24-h -period after treatment. However, previous observations in IVM- and IVO-treated cells demonstrated that the antibiotic exerted a delay in cell-cycle progression and a reduction in the proliferative replication index of both CHO-K1 (Molinari *et al.*, 2009) and *Aedes albopictus* (CCL-126^{TM}) larvae cells (Molinari *et al.*, 2010). Then, these observations could rule out the latter possibility. Previous reports agree with our observations. Cytotoxicity occurs as one of the major consequences of IVM exposure in rat bone marrow cells *in vivo* (el-Nahas and el-Ashmawy 2008) as well as in the absence of a metabolic activating fraction in kidney pig IB-RS-2 cells *in vitro* (Rodriguez and Mattei 1988). Furthermore, it was reported recently that IVM-induced cell death in acute myeloid leukemia cell lines and primary patient samples preferentially over normal hematopoietic cells (Sharmeen *et al.*, 2010).

In our comet assay study, no attempt was made to analyze the frequency of either apoptotic or necrotic cells. Therefore, an increase in the frequency of such types of cells during the latest culture time could also explain the fact that the frequency of comets (slightly damaged and damaged cells) induced by the antiparasiticide is strongly reduced within the 6–24 h after treatment. The results obtained using flow cytometry indicated that IVM and IVO were able to increase not only the frequency of necrotic cells, but in particular those of early- and late-apoptotic CHO-K1 cells with regard to the antibiotic concentration. Moreover, in contrast to experiments analyzing DNA damage, an apoptosis assay was performed on cells continuously exposed to antiparasiticides for 24 h, allowing the accumulation of DNA damage in time. These results suggest that chronic exposure could exceed the cellular potential to repair accumulated DNA damage and consequently redirect cell fate into irreversible apoptosis. Our results are in concordance with our previous observations of decreasing cell viability, the delay of cell-cycle progression and a concomitant reduction of the proliferative rate index in IVM- and IVO-treated CHO-K1 cells (Molinari *et al.*, 2009). Furthermore, the results extend previous observations indicating the ability of IVM to induce confluent necrosis and apoptosis, compatible with drug-induced human liver disease (Veit *et al.*, 2006).

Finally, further *in vitro* study(ies) will be required to reach a better characterization of both genotoxic and cytotoxic effects exerted by IVM and its commercial formulation IVO by employing other cell lines rather than the very-well characterized system CHO-K1 cells. We cannot discard the possibility that in the near future an *in vitro* bioassay will be performed using cell lines in the presence of an activating metabolic system or a metabolic active cell line, such as HepG2 cells.

What is evident from our results is that the decrease in DNA lesions is mostly related to the cytotoxicity exerted by IVM rather than attributable to a repair process of injure introduced into the DNA of CHO-K1-treated cells. Further studies are required to elucidate these findings. However, independently of the events responsible for our results, what is evident is that the damage induced by the antiparasiticide is strongly reduced within the 6–24 h after treatment, associated with the loss of viability.

REFERENCES

Aleksić N, Milutinović M, Bakrač T. 1996. Investigation of the genotoxic effects of ivermectin on human lymphocytes. *Acta Vet. Brno* **46**: 51–55.

Aleksić N, Barjaktarović N. 1993. Investigation on sister chromatid exchange (SCE) by ivermectin. *Genetika* **25**: 219–225.

Burg RW, Miller BM, Baker EE, Birnbaum J, Currie SA, Hartman R, Kong YL, Monaghan RL, Olson G, Putter I, Tunac JB, Wallick H, Stapley EO, Oiwa R, Omura S. 1979. Avermectins, new family of potent anthelmintic agents: producing organism and fermentation. *Antimicrob. Agents Chemother.* **15**: 361–367. DOI: 10.1128/AAC.15.3.361.

Burg RW, Stapley EO. 1989. Isolation and characterization of the producing organism. In *Ivermectin and Abamectin*, Campbell WC (ed.). Springer: New York; 24–32.

Campbell WC, Fisher MH, Stapley EO, Albers-Schönberg G, Jacob TA. 1983. Ivermectin: a potent new antiparasitic agent. *Science* **221**: 823–828. DOI: 10.1126/science.6308762.

Chabala JC, Mrozik H, Tolman RL, Eskola P, Lusi A, Peterson LH, Woods MF, Fisher MH, Campbell WC, Egerton JR, Ostlind DA. 1980. Ivermectin, a new broad-spectrum antiparasitic agent. *J. Med. Chem.* **23**: 1134–1136. DOI: 10.1021/jm00184a014

Egerton JR, Ostlind DA, Blair LS, Eary CH, Suhayda D, Cifelli S, Riek RF, Campbell WC. 1979. Avermectins, new family of potent anthelmintic

agents: efficacy of the B1a component. *Antimicrob. Agents Chemother.* **15**: 372–378. DOI: 10.1128/AAC.15.3.372.

el-Nahas AF, el-Ashmawy IM. 2008. Effect of ivermectin on male fertility and its interaction with P-glycoprotein inhibitor (verapamil) in rats. *Environ. Toxicol. Pharmacol.* **26**: 206–211. DOI: 10.1016/j.etap. 2008.03.011.

Fortini P, Raspaglio G, Falchi M, Dogliotti E. 1996. Analysis of DNA alkylation damage and repair in mammalian cells by the comet assay. *Mutagenesis* **11**: 169–175. DOI: 10.1093/mutage/11.2.169.

González M, Soloneski S, Reigosa MA, Larramendy ML. 2003. Effect of dithiocarbamate pesticide zineb and its commercial formulation azzurro. IV. DNA damage and repair kinetic assessed by single cell gel electrophoresis (SCGE) assay on Chinese hamster ovary (CHO) cells. *Mutat. Res.* **534**: 145–154. DOI.: org/10.1016/S1383–5718(02) 00257–7.

Kita K, Shiomi K, Omura S. 2007. Advances in drug discovery and biochemical studies. *Trends Parasitol.* **23**: 223–229. DOI: 10.1016/j. pt.2007.03.005.

Korystov YN, Mosin VA, Shaposhnikova VV, Levitman MK, Kudryavtsev AA, Kruglyak EB, Sterlina TS, Viktorov AV, Drinyaev VA. 1999. A comparative study of effects of Aversectin C, Abamectin and Ivermectin on apoptosis of rat thymocytes induced by radiation and dexamethasone. *Acta Vet. Brno* **68**: 23–29. DOI: 10.2754/avb199968010023.

Lifschitz A, Virkel G, Ballent M, Sallovitz J, Imperiale F, Pis A, Lanusse C. 2007. Ivermectin (3.15%) long-acting formulations in cattle: absorption pattern and pharmacokinetic considerations. *Vet. Parasitol.* **147**: 303–310.

McGahon AJ, Martín SJ, Bissonnette RP, Mahboubi A, Shi Y, Mogil RJ, Nishioka WK, Green DK. 1995. The end of the (cell) line: methods for the study of apoptosis *in vitro*. *Methods Cell Biol.* **46**: 153–185.

Miller TW, Chaiet L, Cole DJ, Cole LJ, Flor JE, Goegelman RT, Gullo VP, Joshua H, Kempf AJ, Krellwitz WR, Monaghan RL, Ormond RE, Wilson KE, Albers-Schönberg G, Putter I. 1979. Avermectins, new family of potent anthelmintic agents: isolation and chromatographic properties. *Antimicrob. Agents Chemother.* **15**: 368–371. DOI: 10.1128/AAC.15.3.368

Molinari G, Soloneski S, Reigosa MA, Larramendy ML. 2009. *In vitro* genotoxic and cytotoxic effects of ivermectin and its formulation ivomec® on Chinese hamster ovary (CHO_{K1}) cells. *J. Hazard. Mater.* **165**: 1074–1082. DOI: 10.1016/j.jhazmat.2008.10.083

Molinari G, Soloneski S, Reigosa MA, Larramendy ML. 2010. Genotoxic and cytotoxic in vitro evaluation of ivermectin and its formulation ivomec® on *Aedes albopictus* larvae (CCL-126TM) cells. *Toxicol. Environ. Chem.* **92**: 1577–1593.

Olive P, Banáth J, Durand R. 1990. Heterogeneity in radiation - induced DNA damage and repair in tumor and normal cells measured using the comet assay. *Radiat. Res.* **122**: 86–94. DOI: 10.1002/cyto.a.20154

Ŏmura S, Crump A. 2004. The life and times of ivermectin - a success story. *Nat. Rev. Microbiol.* **2**: 984–989. DOI: 10.1038/nrmicro1048.

Ŏmura S. 2008. Ivermectin: 25 years and still going strong. *Int. J. Antimicrob. Agents* **31**: 91–98. DOI: 10116/j.ijantimicag.2007.08.023.

Pitterna T, Cassayre J, Hüter OF, Jung PM, Maienfisch P, Kessabi FM, Quaranta L, Tobler H. 2009. New ventures in the chemistry of avermectins. *Bioorg. Med. Chem.* **17**: 4085–4095. DOI: 10116/j.bmc.2008.12.069.

Rodríguez-Mercado JJ, Mateos-Nava RA, Altamirano-Lozano MA. 2011. DNA damage induction in human cells exposed to vanadium oxides *in vitro*. *Toxicol. In Vitro* 2011; **25**: 1996–2002. DOI: 10.1016/j. tiv.2011.07.009.

Rodriguez MALR, Mattei R. 1988. Toxicity assessment of the antiparasitic ivermectin. *Toxicity Asses.* **3**:379–384. DOI: 10.1002/tox.2540030404.

Sharmeen S, Skrtic M, Sukhai MA, Hurren R, Gronda M, Wang X, Fonseca SB, Sun H, Wood TE, Ward R, Minden MD, Batey RA, Datti A, Wrana J, Kelley SO, Schimmer AD. 2010. The antiparasitic agent ivermectin induces chloride-dependent membrane hyperpolarization and cell death in leukemia cells. *Blood* **116**: 3593–3603. DOI: 10.1182/blood–2010–01–262675.

Singh NP. 1996. Microgel electrophoresis of DNA from individual cells: principles and methodology. In *Technologies for Detection of DNA Damage and Mutation*, Pfeifer GP (ed.). Plenum Press: New York; 3–24.

Sunazuka T, Omura S, Iwasaki S, Ŏmura S. 2003. Chemical modifications of macrolides. In *Macrolide Antibiotics. Chemistry, Biology, and Practice*, Ŏmura S (ed.). Elsevier Inc.: New York; 99–180.

USEPA. 1989. *United States Environmental Protection Agency. Avermectin (Agri-Mek, Affirm) Pesticide Fact Sheet 9/89*. Cornell University: Ithaca.

Veit O, Becka B, Steuerwaldb M, Hatza C. 2006. First case of ivermectin-induced severe hepatitis. *Trans. R. Soc. Trop. Med. Hyg.* **100**: 795–797. DOI: 10.1016/j.trstmh.2006.02.003.

Wei L, Wei G, Zhang H, Wang PG, Du Y. 2005. Synthesis of new, potent avermectin-like insecticidal agents. *Carbohydr. Res.* **340**: 1583–1590. DOI: 10.1016/j.carres.2005.04.019.

Woods DJ, Williams TM. 2007. The challenges of developing novel antiparasitic drugs. *Invert. Neurosci.* **7**: 245–250. DOI: 10.1007/ s10158–007–0055–1.

Yoon YJ, Kim ES, Hwang YS, Choi CY. 2004. Avermectin: biochemical and molecular basis of its biosynthesis and regulation. *Appl. Microbiol. Biotechnol.* **63**: 626–634. DOI: 10.1007/s00253–003–1491–4.

Zhang X, Chen Z, Li M, Wen Y, Song Y, Li J. 2006. Construction of ivermectin producer by domain swaps of avermectin polyketide synthase in *Streptomyces avermitilis*. *Appl. Microbiol. Biotechnol.* **72**: 986–994. DOI: 10.1007/s00253–006–0361–2.